ADAPTIVE EIGENVALUE-BASED SPECTRUM SENSING FOR MULTI-ANTENNA COGNITIVE RADIO SYSTEMS

Christos G. Tsinos and Kostas Berberidis

Dept. of Computer Engineering & Informatics and CTI/RU8, University of Patras 26500, Rio-Patras, Greece,
E-mails: {tsinos,berberid}@ceid.upatras.gr.

ABSTRACT

In this paper adaptive Eigenvalue-Based Spectrum Sensing (EBSS) techniques are proposed for multi-antenna cognitive receivers. In cases where fading channels are involved, and hence real-time processing is required, the adaptive techniques offer lower complexity and exhibit improved performance as compared to the corresponding batch EBSS techniques. At first, novel adaptive EBSS techniques are developed for the Maximum Eigenvalue Detector (MED), the Maximum-Minimum Eigenvalue Detector (MMED), and the Generalized Likelihood Ratio Test (GLRT) schemes, respectively, based on well-studied subspace tracking methods. Moreover, close approximations for the distribution functions of the adaptive test statistics of the MED, MMED and GLRT schemes are derived in order to compute the decision thresholds for a given probability of false alarm. The performance of the adaptive EBSS methods is verified via indicative simulations.

Index Terms— Eigenvalue-Based Spectrum Sensing, Cognitive Radio, Subspace Tracking.

1. INTRODUCTION

Cognitive Radio (CR) provides an efficient way to utilize the available bandwidth in wireless communication systems. The main idea of the CR concept is to allow non-licensed users (Secondary Users - SUs) to transmit their data in a spectrum area that is licensed to the so-called Primary Users (PUs) of the system. To this end, Opportunistic Spectrum Sharing techniques may be employed to optimize the SUs transmissions without degrading the PUs' performance [1].

A common approach is that the SUs establish their communication links only in the so-called "spectrum holes" of the PU system, i.e., to spectrum areas that are temporarily unused by the corresponding PUs. Key role in the aforementioned approaches play the so-called spectrum sensing techniques which are employed by the SUs in order to detect the spectrum holes. The performance of both the PUs and SUs is highly depended on the successful detection of the corresponding spectrum holes and, therefore, a significant part of the recent CR literature is concerned with the design of efficient spectrum sensing techniques.

Several spectrum sensing schemes have been proposed over the last few years including energy-based detectors (EBD), e.g. [2], eigenvalue - based spectrum sensing techniques (EBSS) [3]-[4], covariance - based spectrum sensing techniques [5], and cyclostationary - based spectrum sensing techniques [6]. The EBD methods are usually simple to implement, however, they require knowledge of the involved noise variance. The EBSS methods (particularly, the MMED and GLRT) may operate in a totally blind manner as they do not assume any knowledge concerning the PUs' signals or the noise variance, and also they may offer remarkably improved performance for specific signal categories. However, this is done at the expense of high complexity since they require computation of the Singular Value Decomposition (SVD) of the received signal's sample covariance matrix. Moreover, the computation of the involved decision thresholds is generally based on the asymptotical (limiting) distributions of the corresponding test statistics which, in general, require large number of samples in order to achieve a satisfactory performance. Recently, close approximations for the distribution functions of the test statistics have been proposed in the literature, [7]-[8], though they have quite a complex form. Thus, the computation of the decision thresholds is actually performed by numerical methods which increase even further the computational complexity.

Therefore, mainly due to complexity, the EBSS techniques turn out to be impractical for cases where fast fading channels are involved and on-line signal processing is required. The main goal in this paper is to develop low-complexity adaptive EBSS techniques by relying on well-studied subspace tracking algorithms.

More specifically, the contributions of the present paper are the following ones. At first, novel adaptive EBSS techniques, based on well-known subspace tracking methods, are derived. Note that, to the best of our knowledge, this is the first time that adaptive versions of the EBSS techniques are presented in the literature. Then, the distributions of the adaptive test statistics are derived in order to compute the required decisions thresholds. It turns out that accurate approximations of the test statistics correspond to well-known tabulated functions improving further the practicality of the new adaptive schemes over the batch ones. The proposed adaptive methods are compared with the corresponding batch ones, in terms of performance, for static and fading channels, under different SNR regimes.

The rest of the paper is organized as follows. In Section 2, a brief description is given for the EBSS techniques considered in the present paper. In Section 3, adaptive versions of the EBSS (AD-EBSS) techniques are derived. In Section 4, the test statistics' distribution functions of the proposed AD-EBSS techniques and the corresponding decision thresholds are derived. Section 5 provides some indicative simulations, and Section 6 concludes the work.

2. EIGENVALUE-BASED SPECTRUM SENSING

Let us assume that a single-antenna PU and a SU with R_x antennas are operating in the same frequency band considering a typical interweave CR scheme [9]. The time axis is assumed to be divided into transmit time intervals (time-slots). This time-slot is considered as the basic unit of time scheduling. At the beginning of each PU time-slot (assuming perfect synchronization between the PU and the SU), the SU senses the frequency band, and if no PU activity is detected, then the SU employs the specific time-slot for its transmissions. Let us also assume that during each sensing period the SU obtains N sample vectors $\mathbf{y}_n$, $1 \leq n \leq N$ of dimension $R_x \times 1$. In the associated spectrum sensing problem the following hypothesis test is

This work was supported in part by EU and national funds via the National Strategic Reference Framework (NSRF) - Research Funding Programs: Heracleitus II and Thales (ENDECON), and in part by the University of Patras.

considered,

$$\mathcal{H}_0 : \mathbf{y}_n = \mathbf{z}_n \tag{1}$$

$$\mathcal{H}_1 : \mathbf{y}_n = \mathbf{h}x_n + \mathbf{z}_n, \tag{2}$$

where $\mathbf{z}_n$ is an $R_x \times 1$ additive noise random variable modeled as $\mathcal{CN}\left(0, \sigma_z^2\right)$, $\mathbf{h}$ is the $R_x \times 1$ complex flat channel gain vector between the PU and the SU and x_n is the transmitted PU symbol. That is, under the hypothesis $\mathcal{H}_0$ the PU is idle and the signal $\mathbf{y}_n$ received at the SU contains only noise. On the other hand, under the hypothesis $\mathcal{H}_1$ the PU transmits data and the received SU signal is a superposition of these data (scaled by the channel gain) and noise.

The covariance matrix $\mathbf{R}$ of the signal vectors received at the SU receiver, under the two hypotheses, is given by,

$$\mathbf{R} = \mathbb{E}\{\mathbf{y}_n \mathbf{y}_n^H\} = \begin{cases} \sigma_z^2 \mathbf{I}_{R_x} & \mathcal{H}_0 \\ \sigma_x^2 \mathbf{h}\mathbf{h}^H + \sigma_z^2 \mathbf{I}_{R_x} & \mathcal{H}_1 \end{cases}, \tag{3}$$

where $\mathbb{E}(\cdot)$ denotes the expected value operator, σ_x^2 is the PU's transmitted signal's variance and $(\cdot)^H$ denotes the Hermitian of a matrix. Let us assume that the ordered eigenvalues of matrix $\mathbf{R}$ are denoted by $\lambda_1 \geq \cdots \geq \lambda_{R_x}$. Under the hypothesis $\mathcal{H}_0$, all the latter eigenvalues are due to noise only, that is, $\lambda_1 = \cdots = \lambda_{R_x} = \sigma_z^2$. Under the hypothesis $\mathcal{H}_1$, the first eigenvalue is given by $\lambda_1 = \sigma_1^2 + \sigma_z^2$, where σ_1^2 is the received PU signal's noise power and the rest eigenvalues are given by $\lambda_2 = \cdots = \lambda_{R_x} = \sigma_z^2$. It is clear that the eigenvalues of the covariance matrix can be used to form a sufficient test statistics for the spectrum sensing problem. In the following equations three different test statistics are defined.

$$T^{MED}(\lambda_1) = \frac{\lambda_1}{\sigma_z^2}, \tag{4}$$

$$T^{MMED}(\lambda_1, \lambda_{R_x}) = \frac{\lambda_1}{\lambda_{R_x}}, \tag{5}$$

$$T^{GLRT}(\lambda_1, \ldots, \lambda_{R_x}) = \frac{\lambda_1}{\frac{1}{N-1}\sum_{m=2}^{R_x} \lambda_m}. \tag{6}$$

If the test-statistics' value is above a predefined threshold, a decision in favor of hypothesis $\mathcal{H}_1$ is taken and vice versa. The test statistic T^{MED} is commonly known as the Maximum Eigenvalue Detector and it is proved to be the Generalized Likelihood Ratio Test (GLRT) for the hypothesis testing of Eqs.(1)-(2) under the assumption that only the noise variance is known to the SU ($\mathbf{h}$ and σ_x^2 are unknown) [10]. The test statistic T^{GLRT} is proved to be the GLRT for the previous hypothesis testing assuming also unknown noise variance to the SU [10], [11], [12]. Finally, the T^{MMED} test statistic is commonly known as the Maximum-Minimum Eigenvalue detector and can be considered as a less complex form of the T^{GLRT} one.

In practice, the SU does not know R and computes the sample covariance matrix of the received signals, which is given by,

$$\hat{\mathbf{R}} = \frac{1}{N}\sum_{i=1}^{N} \mathbf{y}_n \mathbf{y}_n^H. \tag{7}$$

The noise eigenvalues of the sample covariance matrix are random variables due to the finite number of samples that are used for its computation. The distribution of these noise eigenvalues is used to compute the decision threshold in a Neyman-Pearson sense for a predefined probability of false alarm. Detailed information on how to compute the decision thresholds is given in [3], [4] and [10].

3. ADAPTIVE EIGENVALUE-BASED SPECTRUM SENSING

The batch EBBS techniques of the previous section are suitable in cases where constant channels during the timeslots and PU-SU perfect synchronization can be assumed. However, if the channels are varying within the timeslot, as it is the case with fading channels, the EBBS techniques are impractical to use due to high complexity (of the regularly required SVD computation) and the fact that they demand a large number of samples as discussed in the Introduction. Indeed, within the sensing period, there is high probability of a deep fading event that could lead to the degradation in the performance of the EBSS techniques. Therefore, the spectrum sensing techniques must be applied more than once within each PU time slot, in order to track the channel variations and avoid a PU "miss-detection" when a deep fading event occurs. In cases where PU-SU perfect synchronization can be assumed, once the SU takes a decision at the end of the sensing period, this decision is valid for the rest of the timeslot since the PU has decided (not) to employ that specific timeslot. That is, even in cases where the involved channels can be assumed constant within the timeslot, if the synchronization assumption is not valid, the SU should be monitoring on a regular basis the spectrum area under consideration in order to detect abrupt changes in the PU system's behaviour.

On-line implementations of the EBSS techniques, capable of tracking the fading channels' variations, can be derived by using low-complexity subspace tracking (ST) algorithms. Several ST algorithms have been proposed in the literature over the past years which are able to track the desired subset of the subspace of a covariance matrix with linear complexity.

In the proposed paper the complex version of the Fast Data Projection Method (FDPM) is employed [13]. The FDPM steps are summarized in the following equations.

$$\mathbf{r}_n = \mathbf{U}_{n-1}^H \mathbf{y}_n \tag{8}$$

$$\mathbf{U}_n = \mathbf{U}_{n-1} \pm \mu \mathbf{y}_n \mathbf{r}_n^H \tag{9}$$

$$\mathbf{U}_n = orth\{\mathbf{U}_n\} \tag{10}$$

$$\mathbf{\Lambda}_n = \alpha \mathbf{\Lambda}_{n-1} + (1-\alpha)|\mathbf{r}_n|^2, \tag{11}$$

where $\mathbf{U}_n$ and $\mathbf{\Lambda}_n$ are the $R_x \times L$ matrix and $L \times 1$ vector that contain the L principal (minor) eigenvectors and eigenvalues, respectively, and α, μ are step size parameters. Note that in equation (9) the sign is a $(+)$ or $(-)$ depending on whether the signal or the noise subspace, respectively, is updated. An orthonormalization procedure is applied in Eq.(10), based on a low complexity Householder transformation [13], and Eq.(11) tracks the corresponding eigenvalues.

For the MED test statistic only the first (maximum) eigenvalue is required, so $\mathbf{U}_n$ is a $R_x \times 1$ matrix and $\mathbf{\Lambda}_n$ is a scalar that contains the current estimate of the maximum eigenvalue. The orthonormalization step is also reduced to a simple normalization one, i.e. $\mathbf{U}_n = \mathbf{U}_n / \|\mathbf{U}_n\|$. In a similar way, the MMED test statistic is estimated. At first, the signal subspace version of the FDPM is employed (with $(+)$ in (9)) to track the maximum eigenvalue and then the noise subspace version follows (with $(-)$ in (9)) to track the minimum one. For the GLRT test statistic the complete FDPM (8)-(11) is used since all the R_x eigenvalues of $\hat{\mathbf{R}}_n$ are required (6).

It is evident now that by employing the FDPM method, the SU is capable of tracking, with low complexity, the value of any of the test-statistics under consideration at every time index within the sensing period. Therefore, once a new signal vector is received, the SU updates the employed test-statistic and decides if a change in the state has been occurred (from $\mathcal{H}_0$ to $\mathcal{H}_1$ and vice-versa). If full synchronization between the PU and the SU slots is assumed the final decision can be taken at the end of the sensing period based on a number of $\mathcal{H}_1$ decisions within the sensing period. That is, if a PU signal is detected in a percentage p of the sensing period then the existence of a PU signal is decided. The percentage p is used to calibrate the $\mathcal{P}_f$ to a desired value. An increase in the value of p results in a decrease

of $\mathcal{P}_f$ and $\mathcal{P}_d$ and vice versa.

In cases where no synchronization between the PU and SU communication is assumed and hence continuous monitoring of the spectrum area of interest is required, the employment of the algorithm presented in Table 1 is proposed. According to Table 1, the SU continuously updates the value of the corresponding test statistics and decides that a change in the state have occurred if the test statistic changes behaviour for a number of N_c consecutive received signals. The parameter N_c is used for calibration of the rate of false alarms and miss-detection events to the desired values. A small value of N_c results in small detection delays and increased rates of false alarm to abrupt changes in the PU behaviour and vice-versa.

Table 1: Adaptive EBSS

Initialization:
The SU detects the present state ($\mathcal{H}_0$ or $\mathcal{H}_1$) by applying the batch EBSS for a sufficient number of received signals, until an initial decision is taken.
for $i = n \to \infty$ **do**
  Update the employed Test-Statistic T via the FDPM (8)-(11)
  if $T \geq \eta, \forall n \in [n - N_c, n]$ under $\mathcal{H}_0$ || $T < \eta, \forall n \in [n - Tc, n]$ under $\mathcal{H}_1$ **then**
    Raise an alarm, change in the state has been detected;
  end if
end for

4. TEST STATISTIC DISTRIBUTIONS AND DECISION THRESHOLDS

In this section, the distribution function of each of the three test statistics Eqs.(4)-(6) is derived for the adaptive case, under the hypothesis $\mathcal{H}_0$, i.e., when no information signal is present in the signal received by the SU. Based on eq.(11) of the FDPM, the distribution functions of the involved test statistics can be tracked at every time index n. The following lemma provides expressions for the aforementioned distribution functions.

Lemma 1 *The distribution functions of the adaptive MED, MMED and GLRT test-statistics updated by eq.*(11) *for a SU of R_x antennas under the hypothesis $\mathcal{H}_0$ can be approximated by the functions,*

$$F_{T^{MED}}(x;\xi,\rho) = \frac{\gamma(\xi x,\rho)}{\Gamma(\rho)}, \tag{12}$$

$$F_{T^{MMED}}(x;\rho) = \mathcal{I}_{\frac{x}{x+1}}(\rho,\rho), \tag{13}$$

$$F_{T^{GLRT}}(x;\rho,R_x) = \mathcal{I}_{\frac{(R_x-1)x}{x+1}}(\rho,(R_x-1)\rho), \tag{14}$$

respectively, where $\xi = \frac{(1-\alpha^n)(1+\alpha)}{((1-\alpha)(1-\alpha^{2n}))}$, $\rho = \frac{(1-\alpha^n)^2(1+\alpha)}{((1-\alpha)(1-\alpha^{2n}))}$, $\gamma(x,\rho) = \int_0^x t^{\rho-1}e^{-t}dt$ is the lower incomplete gamma function, $\Gamma(\rho) = \int_0^\infty t^{\rho-1}e^{-t}dt$ denotes the ordinary gamma function and $\mathcal{I}_x(\rho_1,\rho_2) = \int_0^x t^{\rho_1-1}(1-t)^{\rho_2-1}dt$ is the incomplete beta function.

Proof: Observe that, under hypothesis $\mathcal{H}_0$, the signal vector $\mathbf{y}_n$ received by the SU consists of i.i.d. complex Gaussian noise samples $\mathcal{CN}(0,\sigma_z^2)$. Since matrix $\mathbf{U}_{n-1}$ is orthonormal, the entries $\mathbf{z}_n^{(i)}$ of vector $\mathbf{z}_n = \mathbf{U}_{n-1}^H\mathbf{y}_n$ are also i.i.d. $\mathcal{CN}(0,\sigma_z^2)$. From eq.(11), the $l-th$ eigenvalue of the covariance matrix is estimated as,

$$\lambda_l(n) = \sum_{i=0}^{n}\alpha^i(1-\alpha)|\mathbf{z}_n^{(i)}|^2. \tag{15}$$

According to the previous equation the MED test statistic can be expressed as a weighted sum of chi-squared variables with each one derived by squaring the absolute value of a random variable $\phi_i \sim \mathcal{CN}(0,1)$. A close approximation to the previous distribution can be derived by properly applying the results of [14] to our case. Let us consider the following RV

$$T \triangleq \sum_{i=1}^{m} w_i\zeta_i^2, \tag{16}$$

where $\zeta_i \sim \mathcal{N}(0,1)$ and $w_i \in \mathbb{R}$. Welch, in a 1938 paper [14], proposed an approximation of the distribution of variable T by a scaled chi-squared distribution of ρ degrees of freedom. That is, $T \sim \frac{1}{\xi}\chi_\rho^2$, where $\xi = \frac{\sum_{i=1}^m w_i}{\sum_{i=1}^m w_i^2}$, $\xi = \frac{(\sum_{i=1}^m w_i)^2}{\sum_{i=1}^m w_i^2}$ and the corresponding CDF is given by

$$F_T(x;\xi,\rho) = \frac{\gamma(\xi/2x,\rho/2)}{\Gamma(\rho/2)}. \tag{17}$$

It is now easy to see that, by defining $w_i = \alpha^i(1-\alpha)/2$ and using eq.(17) in the case of complex normal variables ϕ_i, we can apply the previous results to the MED test statistic (4). Moreover, observe that the weights w_i are actually terms of a geometric sequence enabling as to compute closed forms for the parameters ρ and ξ. Thus, it can be easily verified that $\xi = \frac{2(1-\alpha^n)(1+\alpha)}{((1-\alpha)(1-\alpha^{2n}))}$ and $\rho = \frac{2(1-\alpha^n)^2(1+\alpha)}{((1-\alpha)(1-\alpha^{2n}))}$. Finally, by combining these results with eq.(17) the proof for MED is completed.

In the case of the MMED test statistic we seek for the distribution of the ratio of two eigenvalues of matrix $\hat{\mathbf{R}}_n$, that are estimated via Eq.(11). The required distribution is equivalent to the distribution of the ratio $\frac{T^{MED}(\lambda_1)}{T^{MED}(\lambda_{R_x})}$. Therefore, the corresponding CDF is equal to the one of the ratio of two independent T^{MED} random variables. In order to compute the latter CDF, a typical method for the derivation of the ratio of two independent random variables can be followed [15], though the detailed proof is omitted due to space limitations. It turns out that the distribution of the MMED statistic can be approximated by the beta prime distribution with the corresponding CDF given by eq.(13).

Finally, the CDF of the GLRT test statistic can be computed by firstly observing that the random variable $\sum_{m=2}^{R_x}\lambda_m \sim \frac{1}{\xi}\chi^2_{(R_x-1)\rho}$, where the parameters ξ and ρ are defined as in the case of the MED distribution. Then the CDF of the Ratio of the two independent random variables $\frac{\lambda_1}{\sum_{m=2}^{R_x}\lambda_m}$ is computed in a similar way to the MMED test statistic's one. As long as the CDF of the ratio under consideration is computed, it is easy then to compute the CDF of the scaled random variable $T^{GLRT} = \frac{\lambda_1}{\frac{1}{R_x-1}\sum_{m=2}^{R_x}\lambda_m}$ which is given by eq.(14). ∎

As it can be seen from the results of Lemma 1, the CDFs of the adaptive test statistics involve the computation of well-known tabulated functions and the same comment is true for their corresponding inverse functions. The latter observation enables the SU to easily compute the decision thresholds in a Neyman-Pearson sense, for a predefined probability of false alarm $\mathcal{P}_f$, as opposed to the case of the batch test statistics where usually numerical methods are required. To proceed further, first, the decision threshold for the MED test statistic is computed. We equivalently have

$$P_f = P\left\{T^{MED} > \eta^{MED}|\mathcal{H}_0\right\} = 1 - F_{T^{MED}}(x;\xi,\rho) \Rightarrow$$
$$\eta^{MED} = F^{-1}_{T^{MED}}\left(1-P_f;\xi,\rho\right). \tag{18}$$

The decision thresholds for the adaptive MMED and GLRT test statistics can be computed in a similar way, and are given by the following equations,

$$\eta^{MMED} = \frac{\mathcal{I}^{-1}\left(1-P_f;\rho,\rho\right)}{1-\mathcal{I}^{-1}\left(1-P_f;\rho,\rho\right)} \tag{19}$$

$$\eta^{GLRT} = \frac{\mathcal{I}^{-1}\left(1-P_f;\rho,(R_x-1)\rho\right)}{(R_x-1)-\mathcal{I}^{-1}\left(1-P_f;\rho,(R_x-1)\rho\right)} \tag{20}$$

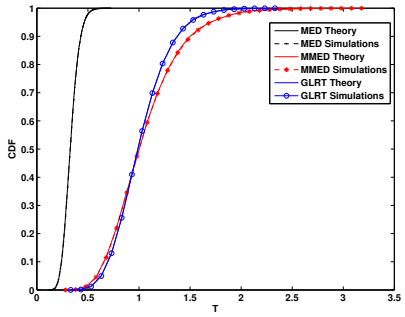

Fig. 1: CDFs of the test statistics under $\mathcal{H}_0$ Eq.(12)-(14)

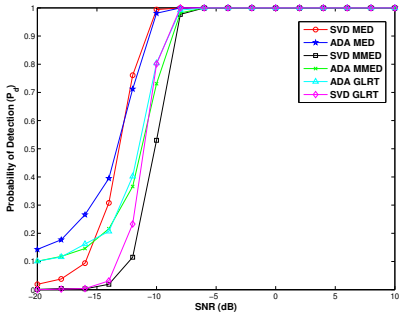

Fig. 2: Probability of Detection ($\mathcal{P}_d$) for static channels

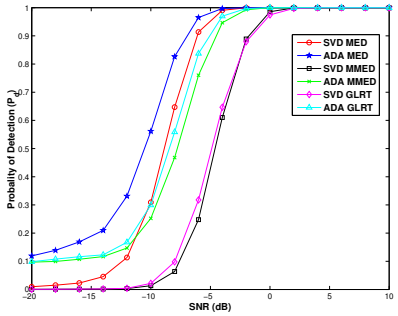

Fig. 3: Probability of Detection ($\mathcal{P}_d$) for fading channels

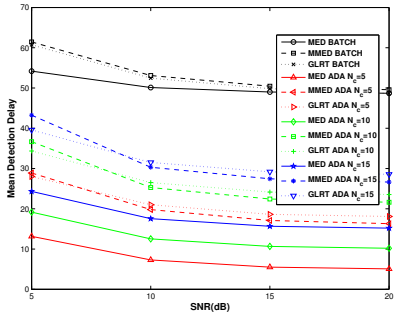

Fig. 4: Mean Detection Delay of an abrupt change

5. SIMULATIONS

In this section, some indicative simulation results are presented in order to evaluate the performance of the adaptive EBSS methods. We assume that the PU transmits a BPSK modulated signal. The step of the FDPM algorithm is set to $\mu = 0.8/\|\mathbf{y}_n\|^2$.

In Figure 1, the theoretical CDFs of the MED, MMED and GLRT adaptive test statistics under the $\mathcal{H}_0$ (Lemma 1) are compared to the empirical ones when a block of $N = 20$ received signal vectors at the SU is used to estimate them. The results of 10000 simulations are averaged so as to compute the empirical CDFs for a SU receiver with $R_x = 4$. As it is shown, the derived theoretical CDFs are very close to the empirical ones even for this small number of received signals.

In Figure 2, the performance of the AD-EBSS techniques is compared to the one of the batch ones in terms of the achieved probability of detection $\mathcal{P}_d$ under different SNR values for probability of false alarm $\mathcal{P}_f = 0.1$. The parameter a of the FDPM algorithm (11) is set to $a = 0.98$. The performance is examined considering constant channels within each timeslot of duration $N = 100$ symbols. The taps of all the involved channels are derived as $\mathcal{CN}(0, 1)$ and the results of 10000 realizations are averaged. The decision of the AD-EBSS techniques is taken at the end of each timeslot. That is, we first examine the performance of the AD-EBSS techniques in a batch sense. Note that, even in the batch approach, the AD-EBSS techniques exhibit reduced complexity compared to the batch ones, as they do not require the computation of the update of the sample covariance matrix given by Eq.(7). As it is shown, the adaptive versions of the test statistics achieve in general close performance to the batch ones (or even better, in some cases). This is due to the fact that the CDFs of the adaptive test statistics Eq.(12)-(14) are close approximations to the exact ones, whereas for the batch case asymptotic expressions are used.

In Figure 3, the same experiment is repeated, though now, time-varying channels are considered. The channels are derived by using a typical Jakes fading simulator with $f_d T_s = 0.01$, where f_d is the Doppler frequency and T_s is the symbol period. Under this fading model, the involved channels are rapidly varying within each sensing period resulting in degradation on the batch detectors performance. In the present simulations, we set $p = 0.18$ for a targeted $\mathcal{P}_f = 0.1$ and $a = 0.8$. As it is depicted, in Fig. 3, the performance of the AD-EBSS techniques is clearly better than the one of the batch ones since the former techniques are able to track the variations of the test statistics within the sensing period (see Section 3).

Finally, in Figure 4 the mean detection delay in an abrupt change is compared for each one of the batch and the adaptive EBSS techniques for different SNR values. We consider timeslots of 1000 symbols in which an abrupt change in the channel state occurred at a random symbol time. The time which a change occurs is assumed to follow a uniform distribution. The batch EBSS techniques are employed for a block of a 100 symbols. That is, at every block the sample covariance matrix is computed and then, the SVD is applied so that the test statistics to be derived. The AD-EBSS techniques are initialized by employing the batch ones for the first 50 received signals in order to determine the initial active hypothesis and then the algorithm of Table 1 is used to update its values. The simulations were derived for $N_c = 5, 10$ and 15 respectively, $a = 0.98$ and $\mathcal{P}_f = 0.01$. As it is shown, the adaptive versions detect the change significantly faster than the corresponding batch ones. Moreover, the probability of false alarm and miss detection events (not depicted due to space limitations) is almost zero for $N_c \geq 10$, for the AD-EBSS, whereas for the batch ones it has always a constant value.

6. CONCLUSION

In this work, adaptive versions of well-known EBSS techniques where developed for multi-antenna cognitive receivers. The proposed adaptive techniques offer low complexity and improved performance when fading channels are considered, i.e., in cases where channel variations degrade the performance of the batch approaches. In order to compute the decision thresholds for each one of the adaptive test statistics, close approximations for the associated distribution functions were derived. The performance of the adaptive EBSS methods was verified via indicative simulations.

7. REFERENCES

[1] S. Haykin, "Cognitive radio: brain-empowered wireless communications," *IEEE Journal on Selected Areas in Communications*, vol. 23, no. 2, pp. 201 – 220, Feb. 2005.

[2] A. Ghasemi and E.S. Sousa, "Collaborative spectrum sensing for opportunistic access in fading environments," in *First IEEE International Symposium on New Frontiers in Dynamic Spectrum Access Networks, DySPAN 2005.*, Nov. 2005, pp. 131 –136.

[3] Y. Zeng, C.L. Koh, and Y.-C. Liang, "Maximum eigenvalue detection: Theory and application," in *Proc, of the 2008 IEEE International Conference on Communications, ICC '08*, May 2008, pp. 4160 –4164.

[4] Y. Zeng and Y.-C. Liang, "Eigenvalue-based spectrum sensing algorithms for cognitive radio," *IEEE Trans. on Communications*, vol. 57, no. 6, pp. 1784 –1793, June 2009.

[5] Yonghong Zeng and Ying-Chang Liang, "Spectrum-sensing algorithms for cognitive radio based on statistical covariances," *IEEE Trans. on Vehicular Technology*, vol. 58, no. 4, pp. 1804 –1815, May 2009.

[6] Mohamed Ghozzi, Francois Marx, Mischa Dohler, and Jacques Palicot, "Cyclostatilonarilty-based test for detection of vacant frequency bands," in *First International Conference on Cognitive Radio Oriented Wireless Networks and Communications*, June 2006, pp. 1 –5.

[7] A. Kortun, T. Ratnarajah, M. Sellathurai, Caijun Zhong, and C.B. Papadias, "On the performance of eigenvalue-based cooperative spectrum sensing for cognitive radio," *IEEE Journal of Selected Topics in Signal Processing*, vol. 5, no. 1, pp. 49 –55, Feb. 2011.

[8] F. Penna, R. Garello, D. Figlioli, and M.A. Spirito, "Exact non-asymptotic threshold for eigenvalue-based spectrum sensing," in *Proc. of the Fourth International Conference on Cognitive Radio Oriented Wireless Networks and Communications, 2009. CROWNCOM '09.*, June 2009, pp. 1–5.

[9] A. Goldsmith, S.A. Jafar, I. Maric, and S. Srinivasa, "Breaking spectrum gridlock with cognitive radios: An information theoretic perspective," *Proc. IEEE*, vol. 97, no. 5, pp. 894 –914, May 2009.

[10] A. Taherpour, M. Nasiri-Kenari, and S. Gazor, "Multiple antenna spectrum sensing in cognitive radios," *IEEE Trans. on Wireless Communications*, vol. 9, no. 2, pp. 814 –823, Feb. 2010.

[11] Pu Wang, Jun Fang, Ning Han, and Hongbin Li, "Multiantenna-assisted spectrum sensing for cognitive radio," *IEEE Trans. on Vehicular Technology*, vol. 59, no. 4, pp. 1791 –1800, May 2010.

[12] B. Nadler, F. Penna, and R. Garello, "Performance of eigenvalue-based signal detectors with known and unknown noise level," in *Proc. of the 2011 IEEE International Conference on Communications (ICC)*, June 2011, pp. 1 –5.

[13] X. G Doukopoulos and G. V Moustakides, "Fast and stable subspace tracking," *IEEE Trans. on Signal Processing*, vol. 56, no. 4, pp. 1452–1465, Apr. 2008.

[14] B. L. Welch, "The significance of the difference between two means when the population variances are unequal," *Biometrika*, vol. 29, no. 3/4, pp. pp. 350–362, 1938.

[15] A. Papoulis, *Probability, Random Variables, and Stochastic Processes*, 3rd edition, 1991.